Combined LH and ECH Experiments in the FTU Tokamak

V. Pericoli Ridolfini, Y. Peysson[1], R. Dumont[1], G. Giruzzi[1], G. Granucci[2], L. Panaccione, L. Delpech[1], B. Tilia, FTU team, ECH team[2]

Associazione Euratom-ENEA sulla Fusione, C.R. Frascati, 00044 Frascati (Roma)-Italy
e-mail contact of main author: pericoli@frascati.enea.it

Abstract. The effects of the simultaneous injection of LH, up to 1 MW, and ECH power, up to 0.75 MW, have been studied in FTU. In the absence of the cold EC resonance in the plasma (B_T=7.2 T), the suprathermal electron tail generated by LHCD absorbs the ECH power effectively, up to 80%. In a restricted parameter range, additional electron heating due to ECH waves (up to 1.2 keV for P_{ECH}=0.7 MW) is also observed. With the cold resonance at the centre (B_T=5.3T) and no absorption on the tail, the ECH power injection into a sawteeth and MHD free plasma, fully sustained by LHCD, causes a quasi-stationary large increase of the electron temperature in a region r/a<0.5, with T_{e0}>4keV for P_{ECH}=0.35 MW only. This strong heating exceeds the predictions of the mixed Bohm/gyro-Bohm model with magnetic shear correction, which, instead reproduces the LH phase well.

1.- Introduction

In FTU (Frascati Tokamak Upgraded) we began to study the effect of the simultaneous application of the two main electron-heating methods available on tokamak plasmas, the lower hybrid (LH) and the electron cyclotron (EC) radio-frequency waves. The motivation is to try to combine their most appealing features, respectively the high current drive (CD) efficiency and the very localised power deposition. An efficient and localised absorption of the EC power by the LH fast electron (e⁻) tail would mean a significant progress towards a fine steady control of the current radial profile j(r), crucial for advanced tokamak operations. On the other hand, central EC heating (ECH) of the bulk e⁻ is a promising way towards a stable high performance regime in a full LH current driven (LHCD) plasma, where good transport properties are established by the reversed shear profile of the safety factor q(r) [1]. Indeed, the absence of the toroidal electric field breaks the link between j(r) and T_e(r), and it does not allow q(r) to change under strong e⁻ heating, at first approximation. In addition, further EC heating of the 'hot' e⁻ tails can produce a synergetic increase of the global CD efficiency [2,3], and it can extend the range of B_T (toroidal magnetic field) useful for ECH in the downshifted frequency scheme [4], where the resonance condition for the e⁻ tails requires a B_T value higher than the cold one, to compensate for the relativistic mass increase.

The above scenarios, i.e. ECH of the hot e⁻ tails or of the central low energy e⁻ in a full LHCD plasma, have both been studied in FTU and are here described. In contrast to similar experiments on other tokamaks [5-8], FTU operates at more reactor relevant plasma densities and injected power: up to P_{LH}=900 kW (f_{LH}= 8 GHz), and P_{ECH}=750 kW (f_{ECH}= 140 GHz) have been simultaneously coupled at line averaged density n_e 0.8·10²⁰ m⁻³. More importantly, the investigation has been carried out in quasi a steady-state CD phase, instead of current ramp-up conditions, as in Ref. [5-7].

The paper is organised as follows. The experimental conditions and results are presented in Sec. 2. Comparison with theory is discussed in Sec. 3. In Sec. 4 conclusions will be drawn.

2. Experiment

2.1 ECH waves absorption by LH generated fast electron tails
We chose a sufficiently high central magnetic field (B_{T0}=7.2 T) in order to remove any interaction with the bulk electrons, and to simplify the interpretation. In this down-shifted scheme, the cold resonance, at B_T^*= 5 T, is well outside the vacuum vessel (major radius R=0.93 m, minor radius a=0.3 m), whereas resonance with the LH fast electrons takes place
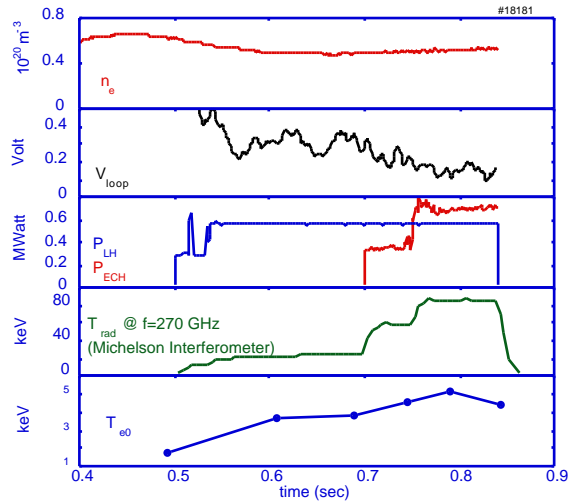
FIG. 1 - #18181, B_T=7.2T, time evolution of 1) line density; 2) loop voltage; 3) coupled LH and ECH power, 4) radiation temperature of the suprathermal e^- 5) central electron temperature
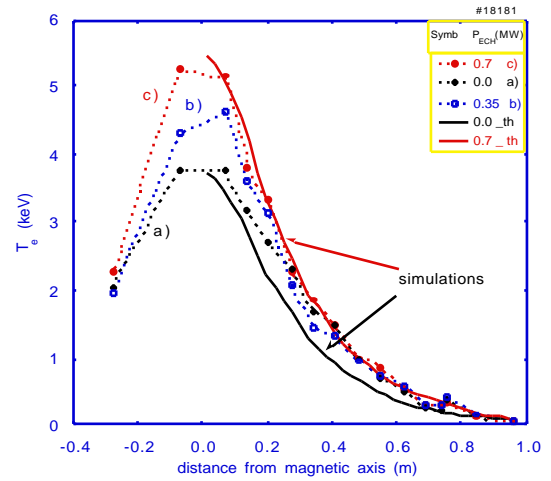
FIG. 2 - #18181 profiles of the electron temperature. Solid symbols, experiment: a) LH only, b) P_{EC}= 0.35 MW; c) P_{EC}=0.7 MW. Full lines Computation for cases a) and c)

for: $B_T/B_T^* = (n_{||}-N_{||})/(n_{||}^2-1)^{1/2}$ [3]. $N_{||}$ and $n_{||}$ are the parallel indexes of refraction respectively of the LH and ECH waves, and the e^- tail has a velocity =$c/n_{||}$ (c= light speed).

Although this regime could be optimised by an appropriate choice of $N_{||}$, we fixed $N_{||}$=0, and the polarisation of the ECH waves to the O-mode, as a first step and as a reference. The $n_{||}$ was fixed at 1.52 the minimum value for a reliable coupling in FTU, in order to maximise the extension of the interacting region. We tried also different $N_{||}$ and $n_{||}$ as well as the X-mode polarisation, as discussed below, but a systematic investigation of such scenarios is postponed to the next experimental campaign. The ECH absorbed power fraction, $_{ECH}$, is deduced from the signals of two probes, at different locations inside the FTU vessel, which detect the escaping ECH power, integrating over all the transits of the waves across the plasma [9].

The effects of P_{ECH} on the fast e^- tail are observed on the hard X-ray (HXR) (photon energy = 20-200 keV) and EC emission (ECE) spectra, with a camera[3][10], viewing along 17 chords across the whole FTU cross section, and with a Michelson interferometer respectively.

In all the explored plasma densities and currents $_{ECH}$ is always 40% (and up to 80%), and the effects on the ECE and HXR signals are significant. These latter in particular, give the perpendicular photon temperature, $T_{,ph}$, increasing from about 15 to 25 keV, which is a clear feature of the direct interaction of the EC waves with the fast e^- tail. On the other hand, macroscopic effects on T_e are observed only when the LH hot e^- tails are bounded to /a 0.3, according to the HXR emission radial profiles, $f_{HXR}(r)$, and when $\bar{n}_e$ 0.5·10^{20} m^{-3}. Fig.1 shows, as an example, the time evolution of the main plasma quantities. In Fig. 2 are plotted the experimental T_e profiles, with LHCD only (P_{LH}=0.6 MW) and when P_{ECH}= 0.35 and =0.7 MW is also injected, together with those predicted by transport code simulations, as described in Sec. 3.1. The e^- temperature increase extends all over a region with r<10 cm (=0.3), it reaches the value of 1.2 keV at the centre, and it is clearly correlated to P_{ECH}. The drop of the loop voltage, V_{loop}, from 0.32 to 0.12 V, during the ECH pulse, implies an increment of the driven current $I_{p,ECH}$ 90 kA, [12]. This value reduces to 30 kA when V_{loop} is led to near 0, indicating a non negligible effect of the residual electric field. The ECH waves, perpendicularly injected, do not carry any momentum: $I_{p,ECH}$ can increase only due to the further reduced fast e^- collisionality, therefore a not large value is expected in any case. The described effects start to decrease beyond the limits of the parameter range specified

---

[3]The HXR camera is on loan at FTU from TORE SUPRA, CEA-Cadarache, France, within the frame of an official collaboration on the issue of the study of the current profile control with LHCD
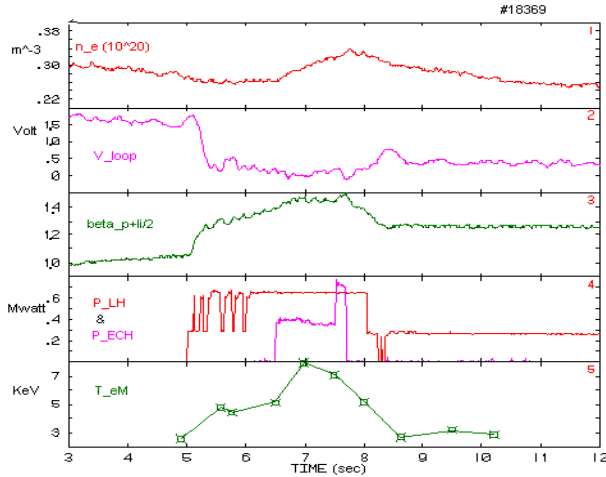
FIG. 3 - #18369, B_T=5.3 T. Time evolution of: 1) line density; 2) loop voltage; 3) poloidal beta + l_i/2; 4) coupled LH and ECH power, 5) electron temperature on the point closest to the magnetic axis (r=3 cm, Thomson scattering).
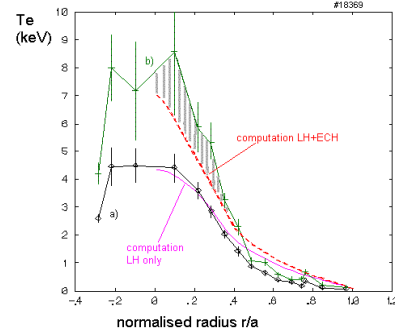

FIG. 4 – #18369. Temperature profiles: Symbols: experimental; lines: computation. a): LH only, P_{LH}=0.6 MW; b): LH+ECH, P_{ECH}=0.35 MW. The shadowing marks the difference between model and experiment

above, more rapidly for T_e and V_{loop} than for the direct suprathermal signatures on the ECE and HXR diagnostics. We attribute this to the limited LH and ECH power at present available. At larger radii the ECH power is deposited in a less confining region and spread over a greater volume. Its local absorbed density then can become too small, just as it occurs when shifting outwards the cold resonant layer in FTU standard ECH operation [11]. At higher density, instead, the electron heating efficiency is reduced mostly by the increased ion-e⁻ collisionality: the power losses rise and the number of LH fast e⁻ decreases as $1/n_e$, causing a less localised power absorption. Quantitative assessment of these effects is in progress.

2.2 ECH central heating of full LHCD plasmas with no MHD activity

The target plasma for the experiments at B_T=5.3 T was chosen in order to maximise the heating effects. Two main constraints, i.e.: 1) low plasma density to minimise collisionality, 2) LH power high enough to stabilise the MHD activity but still comparable to the available ECH power, imposed the following parameters: $\bar{n}_e$ 0.4·10²⁰ m⁻³, P_{LH} 600 kW, I_p=350 kA. In Fig. 3, the time evolution of the main plasma quantities is shown, and in Fig. 4, the radial profiles T_e(r) during the LH only and the LH+ECH phase are plotted. When the ECH power is injected, T_e increases inside a wide region, r 15 cm, 0.5, and jumps from about 4 to 8 keV at the peak. Extrapolation to the magnetic axis gives T_{e0}>10 keV. Despite the large T_e(r) modification no MHD activity or sawteeth develop during the ECH phase, in agreement with an expected small modification of j(r). Accordingly, f_{HXR}(r) and T ph are substantially unchanged, as well as the q(r) profile, as given by the magnetic measurements, which shows an almost flat shear over a wide region. The constancy of T ph is a clear sign that no direct interaction between the ECH waves and the current carrying e⁻ is taking place. This regime appears as quasi stationary according to all our diagnostics. A further increase of T_{e0} occurs during the short interval when P_{ECH} is doubled, according to the p behaviour. As discussed in the next section, an improved electron transport is probably obtained in this regime.

3. Comparison theory – experiment

3.1 ECH waves absorption on LH generated fast electron tails

Comparison with theory is made on: i) absorption of the ECH waves, ii) CD efficiency and profile control, iii) transport analysis. A model combining 3-D Fokker-Planck with current and heat transport simulations [13] is used to determine the 3-D tail structure simultaneously with the T_e and q profiles. In this model, the LH wave spectrum inside the plasma is bounded by the propagation domains [14]. Coupled heat and current transport is computed by the ASTRA code [15], using the mixed Bohm/gyro-Bohm model for the heat diffusivity, with an appropriate shear function [1], which connects T_e and q profile evolutions. Once the tail structure is computed, the absorption of the ECH waves by the tail is evaluated, together

with the additional effect on the driven current and on the diagnostics sensitive to the fast e⁻, in particular non-thermal ECE.

i) Absorption - In order to match the experimental value of η_{ECH}, 70%, a multiple pass of the ECH waves across the plasma core must be admitted. The reflection on the walls is modelled as a non-specular one, after which both directivity and polarisation of the waves are lost. Fig. 5 compares the computed ECE spectra with the measured ones. On the other hand, considering only the first-pass damping, produces a very narrow peak around f 270 GHz, in strong disagreement with the experimental spectrum during the ECH phase. These measurements, performed systematically for this first scenario, give the expected dependence of η_{ECH} on the main parameters: $\bar{n}_e$, P_{LH}, ECH polarisation, and magnetic field. As an example Fig. 6 plots η_{ECH} versus $\bar{n}_e$: the inverse proportionality to n_e of the e⁻ fast population causes an almost linear decrease of η_{ECH}, as well as its increase with P_{LH}, not shown here. Changing the polarisation from O to X mode η_{ECH} grows from 67% to 80% with an error of about ±9% against computed single pass values of 25% and 40%, respectively.

ii) CD efficiency and profile - Upon changing B_T from 7.2 to 6.9 T, we observe an increase of η_{ECH} from 76% to 80% ±6%, and of $I_{p,ECH}$ from 30 to 70 kA approximately, together with a peaking of the high energy part of $f_{HXR}(r)$, and of $j(r)$ accordingly. The peaking of $j(r)$ is deduced from the reconstructed $q(r)$ profiles, whereas that of the HXR, from the ratio between the fluxes along two viewing chords, the central to a peripheral one (impact parameter p=14 cm, =0.48). This ratio is shown in Fig. 7 for energies E_{ph}>160, 120, and 60 keV, together with density, LH and ECH power. The physical reasons for these effects can be understood following Ref. [3]. They are the larger extension of the interacting region, slightly prolonged beyond the plasma centre at 6.9 T, and the variation of the resonance radius for the different energy components of the e⁻ tail: the fastest ones are brought into resonance just at the centre, and this can justify the peaking of the HXR highest energy component.
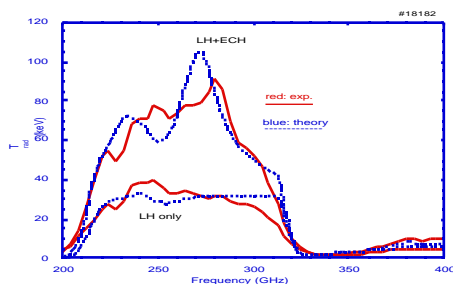

FIG. 5 – #18182, B_T=7.2 T: Experimental and calculated spectra of the radiation temperature, during the LH only and LH+ECH phase for strong interaction of ECH power with the fast e⁻ tails.
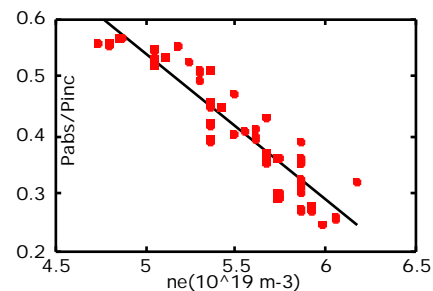

FIG. 6 – Absorbed ECH power fraction versus _n_e when the interaction with the LH fast electron tail only is possible, B_T=7.2 T, P_{LH}=0.6 MW, P_{ECH}=0.7 MW
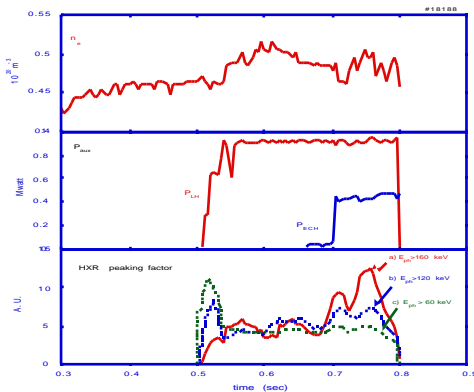

FIG 7 – # 18188: time evolution of 1) n_e ; 2) P_{LH} and P_{ECH}; 3) HXR peaking factors [a),b),c): E_{ph}>60,120,160 keV]
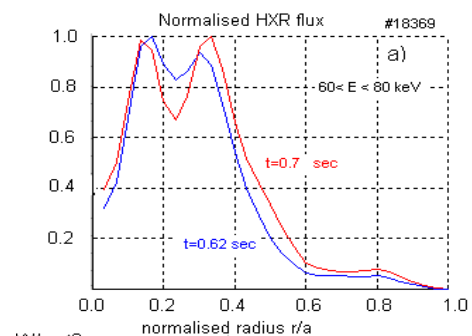

FIG. 8 – # 18369: HXR profile during the LH only and LH+ECH phase. No significant change occurs upon ECH injection

iii) Transport - The transport analysis showed that with the constraint $\eta_{ECH} \geq 0.7$ the absorption processes are well modelled. Indeed, Fig. 2 shows that the radial profiles $T_e(r)$ are reasonably well reproduced.

3.2 ECH central heating of full LHCD plasmas with no MHD activity. The transport analysis for the shot shown in Fig 3 has been performed using the profiles of the HXR spectra at energies of 60-80 keV for both the absorbed power and the driven LH current. This is a good approximation, as discussed in Ref [16]. The Fokker-Planck equation is not used to recompute the distribution function when ECH power is applied, because no interaction with the fast e⁻ tail takes place, as pointed out in the previous section. Fig. 4 shows that $T_e(r)$ can be reproduced well in the LH only phase, whereas the temperature increase is underestimated in the LH+ECH phase, if the same transport model is used. On the other hand, all the information we rely on, indicate that no significant change of either the LH or ECH power deposition is occurring during the LH+ECH phase, as compared with the LH only phase. They come from $f_{HXR}(r)$, shown in Fig. 8, from the LH power deposition calculated with a ray tracing + Fokker-Planck code, from q(r), and from T_{ph}. This temperature profile is therefore consistent with the onset of an internal transport barrier, even though no increase of the global confinement time over the usual L-scaling laws still takes place.

4. Conclusions

The FTU results extend the evidence of absorption of ECH waves on the fast electron tails generated by the LH waves to more interesting and reactor relevant regimes and to quasi stationary conditions, as compared with previous experiments [5,6,7]. The absorption process is quite efficient. Macroscopic effects on the temperature are also observed. Increase of the driven current, and the possibility of the current profile control have been proved. Agreement with theory is satisfactory, even if still semi-quantitative on some points.

The experiment of launching ECH power in a fully MHD and sawteeth free plasma, sustained by LHCD, has demonstrated that a stable and high performance plasma can be obtained in this way. Indeed no important modification of the current profile is undergoing when heating with ECH power, because of the absence of the electric field. The high T_{e0} ($\approx$ 8 keV) and the large increase of the temperature profile inside half radius ($\Delta T_{e0} \approx$ 4 keV for only 0.35 MW of ECH power, could not be fully reproduced by the transport codes using the Bohm/gyro-Bohm model. Therefore, an additional model for confinement improvement should be identified and confirmed by investigations to be performed in future experiments.

References
[1] VLAD, G. et al., Nucl. Fusion **38** (1998) 557
[2] FIDONE, I., et al., Nucl. Fusion **27** (1987) 579
[3] D. FARINA, D., POZZOLI, R., Phys. Fluids B **1** (1989) 1042
[4] FIDONE, I., et al., Phys. Fluids **27** (1984) 661
[5] ANDO et al., Phys. Rev. Lett. **56** (1986) 2180
[6] YAMAMOTO et al., Phys. Rev. Lett. **58** (1987) 2220
[7] MAEKAWA et al., Phys. Rev. Lett. **70** (1993) 2561
[8] CÔTÉ, A., et al., Proc. 25th EPS Conf. on Controlled Fusion and Plasma Physics, Praha, Czech Republic, 29 June – 3 July 1998,.**22C** (1998) 1336
[9] NOWAK, S., et al., to be published in Fusion Engeen.
[10] PEYSSON, Y., IMBEAUX, F., Rev. Sci. Instrum. **70** (1999) 3987
[11] CIRANT, S. et al., Radiofrequency Power in Plasmas, (13th Top. Conf. on RF Power in Plasmas, Annapolis, USA 1999), p. 221, American Institute of Physics, New York (1999)
[12] PERICOLI RIDOLFINI, V., et al., Phys. Rev. Lett. **82** (1999) 93
[13] DUMONT, R., et al., Phys. Plasmas **7** (2000) December issue
[14] BARBATO, E., Plasma Phys. Contr. Fusion **40** (1998).A63
[15] PEREVERZEV, G.V., et al., Nucl. Fusion **32** (1992) 1023
[16] PEYSSON, Y., Radiofrequency Power in Plasmas, (13th Top. Conf. on RF Power in Plasmas, Annapolis, USA 1999), p. 183, American Institute of Physics, New York (1999)